molecular pharmaceutics

Article

pubs.acs.org/molecularpharmaceutics

Ex Vivo Detection of Iron Oxide Magnetic Nanoparticles in Mice Using Their Intrinsic Peroxidase-Mimicking Activity

Jie Zhuang,[†] Kelong Fan,[†] Lizeng Gao,[†] Di Lu,[†] Jing Feng,[†] Dongling Yang,[†] Ning Gu,[‡] Yu Zhang,[‡] Minmin Liang,*[,†] and Xiyun Yan*[,†]

[†]Key Laboratory of Protein and Peptide Pharmaceutical, National Laboratory of Biomacromolecules, CAS-University of Tokyo Joint Laboratory of Structural Virology and Immunology, Institute of Biophysics, Chinese Academy of Sciences, 15 Datun Road, Beijing 100101, China

[‡]State Key Laboratory of Bioelectronics, Southeast University, Nanjing 210096, China

Supporting Information

ABSTRACT: Iron oxide magnetic nanoparticles (MNPs) are widely used as diagnostic and therapeutic agents for biomedical applications. Quantitatively analyzing biodistribution, pharmacokinetics and organ clearance of MNPs in mouse models is important for understanding their in vivo behavior. In this study, we developed a novel histochemical method for visualizing unlabeled MNPs in mouse tissues by employing their intrinsic peroxidase-mimicking activity, regarding which we reported previously that MNPs could catalyze the oxidation of peroxidase substrates to produce a color reaction at the site of MNPs (Gao et al. *Nat. Nanotechnol.* **2007**, *2*, 577−583[1]). Based on this MNPs-peroxidase approach, we determined the biodistribution and organ clearance of MNPs by visualizing and quantifying the localization of MNPs within the main organs. Compared to traditional Prussian blue assay, this novel MNPs-peroxidase approach has higher sensitivity. In conclusion, the developed MNPs-peroxidase approach based on intrinsic peroxidase activity of iron oxide nanoparticles was used effectively for quantitative detection of MNPs in mice by histochemical staining. Presumably, other nanoparticles having intrinsic peroxidase activity could also be considered.

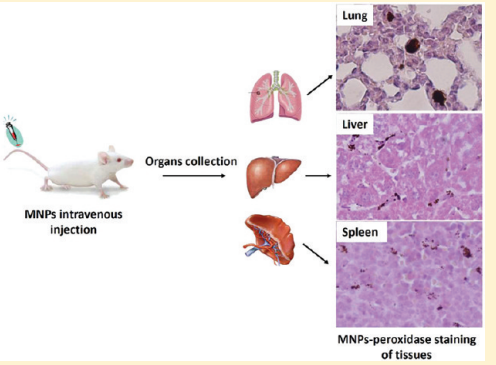

KEYWORDS: *iron oxide magnetic nanoparticle, peroxidase-mimicking activity, biodistribution, organ clearance*

INTRODUCTION

Iron oxide magnetic nanoparticles (MNPs) hold promise as diagnostic, therapeutic and theranostic agents for a wide variety of human diseases, for example as transporters for drugs or as contrast agents.[2−4] To render MNPs viable for clinical translation, it is essential to understand their behavior after administration into the body. However, sensitive detection of MNPs in mice is difficult because nanoparticle behavior is a complex functions of the surface physicochemical properties, hydrodynamic diameter, solubility, stability, shape and flexibility.[5,6] Moreover, the endogenous iron in the form of iron-containing proteins (e.g., hemoglobin, transferrin, and ferritin) may also interfere with low tissue concentrations of MNP detection. In the past several years, many optical and radioisotopic indicators have been conjugated to iron oxide nanoparticles as molecular imaging agents for assessing the biodistribution and pharmacokinetics of MNPs in mice.[7−9] However, exogenous labeling is likely to change the surface properties of nanoparticles and affect their in vivo pharmacokinetics and tissue distribution. In addition, the unavoidable detachment of labels from nanoparticles in serum often causes false detection results, especially when MNPs need long-term monitoring because of their slow clearance from the body.[10,11] Therefore, developing a method by employing their intrinsic properties to achieve nanoparticle detection in mice will be more advantageous. The ex vivo Prussian blue histological staining is a convenient assay to detect the presence of MNPs in mouse organs by using their intrinsic chemical properties.[12−14] However, Prussian blue staining is not sensitive enough to detect low amounts of iron in tissues. In addition, the staining results are usually affected by endogenous ferric iron in tissues.[15]

In previous studies, we first reported that ferrimagnetic nanoparticles exhibit peroxidase activity that can catalyze the oxidation of peroxidase substrates in the presence of H_2O_2 to produce a color reaction, similar to that of natural peroxidases.[1] Since reported in 2007, this finding has been widely applied in medicine, biotechnology and environmental chemistry biotechnology.[16−21] In this study, we developed a MNPs-peroxidase method based on the intrinsic biochemical property

Received: January 18, 2012
Revised: April 11, 2012
Accepted: May 24, 2012

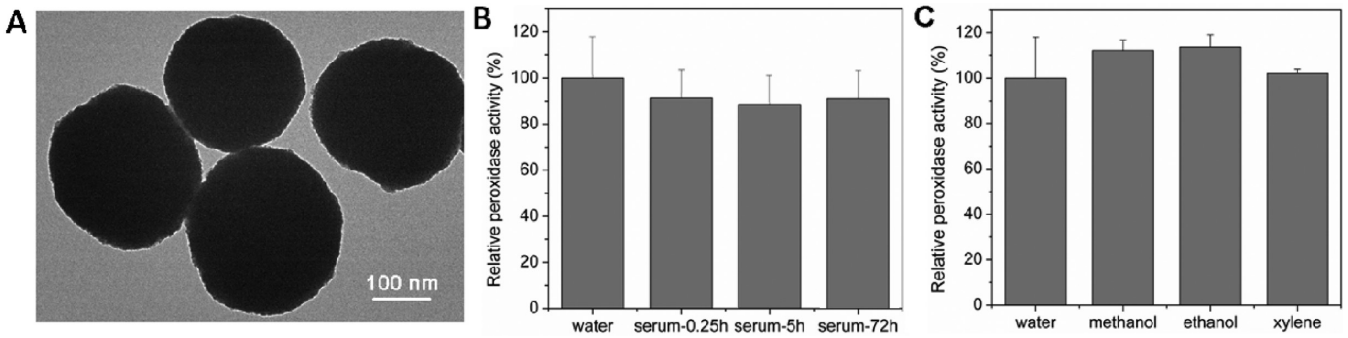

Figure 1. Characterization of dextran-coated MNPs. (A) TEM images of dextran-coated MNPs. (B) Stability of peroxidase activity of dextran-coated MNPs in 70% normal mouse serum at 37 °C over 72 h or (C) in organic chemical reagents at 25 °C over 1 h. $P > 0.05$ from water incubation control; $n = 3$ per group.

of nanoparticles and investigated the biodistribution and organ clearance of MNPs in mouse models.

MATERIALS AND METHODS

Nanoparticle Synthesis and Characterization. Dextran-coated MNPs were synthesized according to the hydrothermal method with some modification.[22] Briefly, $FeCl_3 \cdot 6H_2O$ was dissolved in ethylene glycol, followed by addition of NaAc and dextran. The mixture was stirred vigorously for 30 min, then sealed in an autoclave, and heated at 200 °C for 30 h. The products were collected by washing several times with ethanol and dried at 60 °C.

Silica-coated MNPs were prepared following the Stöber method.[23] Briefly, a solution of base (10 M NaOH) was mixed with iron salts at a molar ratio ($FeCl_2$:$FeCl_3$) of 1:2. The mixture was stirred for 1 h at 20 °C and then was heated at 90 °C for 1 h. The iron oxide dispersion was stirred for 30 min at 90 °C upon addition of 200 mL of trisodium citrate solution (0.3 M). The ultrafine magnetic particles were precipitated with acetone, and the supernatant was decanted by a magnet. Subsequently, water was added to redisperse ultrafine magnetic particles. The resultant dispersion was treated by dialysis and adjusted to 2.0 wt %. The obtained magnetite dispersion was then homogenized by ultrasonic vibration in a water bath. Under continuous mechanical stirring, tetraethoxysilane was slowly added. After 12 h of stirring, silica was formed on the surface of magnetite nanoparticles through hydrolysis and condensation of tetraethoxysilane.

A peroxidase activity test was carried out on dextran-coated MNPs and silica-coated MNPs at room temperature. Dextran-coated or silica-coated MNPs (20 μg) were first mixed with 500 mM H_2O_2 in sodium acetate buffer (pH 3.5), using 3,3,5,5-tetramethylbenzidine (TMB, Sigma) as the substrate. Color reactions were recorded 30 min after the addition of substrate.

MNP Biodistribution and Clearance Study. Male Balb/c mice (6−8 weeks old) were purchased from the Institute of Materia Medica, Chinese Academy of Medical Sciences. All animal studies were performed with the approval of the Chinese Academy of Sciences Institutional Animal Care and Use Committee. Mice were intravenously administered with 10 mg/kg of dextran-coated MNPs or silica-coated MNP to evaluate organ distribution of MNPs ($n = 4$ mice per group). PBS-administered mice were used as control. At 0.25, 5, and 72 h postinjection, mice were sacrificed. Organs of interest (liver, spleen, lungs, kidneys, lymph node and thymus) were collected, fixed and embedded in frozen or paraffin sections for subsequent histological staining.

The tissue location of MNPs were evaluated by staining tissue sections using MNPs-peroxidase assay. Paraffin-embedded tissue sections were first deparaffinized by washing twice in xylene for 10 min and then hydrated progressively in an ethanol gradient. Endogenous peroxidase activity was quenched by incubation with 0.3% H_2O_2 in methanol for 30 min. Freshly prepared DAB was added for color development. The staining was stopped by rinsing sections with double-distilled water. Tissue sections were finally counterstained with hematoxylin. Frozen tissue sections were incubated with 0.3% H_2O_2 to quench endogenous peroxidase activity and then stained with DAB to develop color. After rinsing with water, tissues were counterstained with hematoxylin. Stained tissues were imaged under an Olympus microscope and quantified using ImageJ software.

Prussian Blue Staining. Paraffin-embedded tissues from MNP-administered mice were stained by Prussian blue staining solution (a mixture of 20% hydrochloric acid and 10% potassium ferrocyanide solution in a 1:1 volume ratio) and then washed gently with PBS. Tissues were also counterstained with hematoxylin and eosin (H&E) staining.

Data Analysis. Quantitative data are expressed as means ± SD. Means were compared using one-way ANOVA and Student's t test. P values of <0.05 were considered statistically significant.

RESULTS

Intrinsic Peroxidase Activity of MNPs. To date a wide variety of MNPs have been synthesized, differing in size (hydrodynamic diameter varying from 10 to 500 nm) and type of coating material used, such as dextran, silica, albumin, polyethylene glycol, gold and liposomes.[24−26] Among various types of coating materials, natural polymers, in particular dextran, are the most popular for coating MNPs because of their biocompatibility and simple coating protocols.[27−29] Therefore, dextran-coated MNPs were selected as representative for this investigation.

The synthesized dextran-coated MNPs were first analyzed by transmission electron microscope (TEM). As shown in Figure 1A, nanoparticles were monodispersed and evenly distributed in size with an average diameter of 300 nm. We then characterized the peroxidase activity of dextran-coated MNPs in serum and in organic solutions. Serum incubation at 37 °C was used to test the stability of peroxidase activity of MNPs in circulation in mice. Organic solutions, including ethanol, methanol and xylene, were used for MNP incubation to test the in vitro stability of peroxidase activity of MNPs because

dx.doi.org/10.1021/mp300033a | Mol. Pharmaceutics XXXX, XXX, XXX−XXX

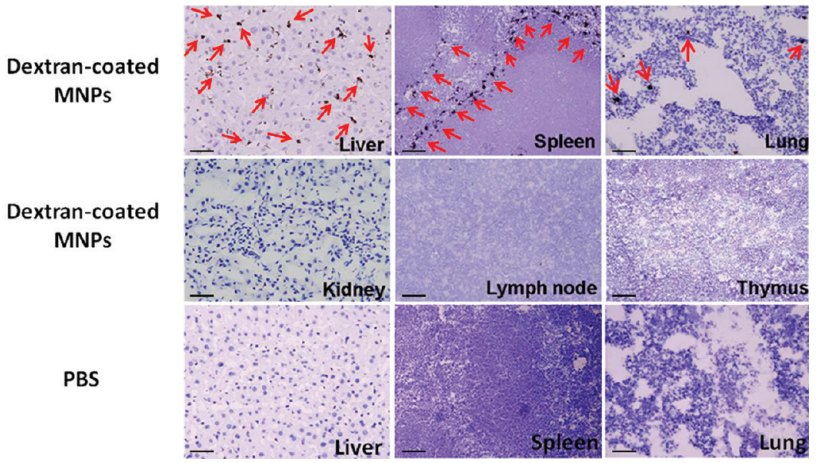

Figure 2. MNPs-peroxidase staining of frozen liver, spleen, lung, kidney, lymph node and thymus from dextran-coated MNP-administered mice or PBS-administered mice. Arrows indicate stained MNPs. (Scale bar = 100 μm.)

tissue slides located with the MNPs will be treated by these chemical reagents during the tissue staining process. After incubation in serum or organic solutions, MNPs were separated using a magnet and then mixed with TMB substrate for color formation. Peroxidase activity of MNPs was indicated by measuring the formed color intensity. As shown in Figure 1B,C, the peroxidase activity of dextran-coated MNPs did not show a substantial change, suggesting peroxidase activity stability over this period. We next compared the peroxidase activity of commercially available dextran-coated MNPs with our laboratory synthesized dextran-coated MNPs. As shown in Supplementary Figure S1 in the Supporting Information, commercial MNPs at the same size exhibited the similar peroxidase activity with our synthesized MNPs under the same conditions, illustrating that there are no limitations to MNP sources.

Biodistribution of MNPs. By utilizing the peroxidase activity of magnetic nanoparticles that can catalyze the oxidation of peroxidase substrates to form a color deposition at the site of MNPs, we evaluated the organ biodistribution of dextran-coated MNPs in mice. Four mice each intravenously received an injection of 10 mg/kg of MNPs and then were sacrificed at 5 h postinjection. PBS-administered mice were used as control. Organs including liver, spleen, lung, kidney, heart, lymph node and thymus were harvested and embedded in frozen sections and stained with MNPs-peroxidase assay using DAB as staining substrate. As shown in Figure 2, the dextran-coated MNPs can catalyze the oxidation of DAB in the presence of H_2O_2 and form an insoluble brown deposition at the sites of MNPs. To quantify the accumulated MNPs in these tissues, ten representative tissue slices were randomly chosen from the same tissue. The accumulated MNPs per area of these representative slices were analyzed by the ImageJ. As shown in Supplementary Figure S2 in the Supporting Information, dextran-coated MNPs were mainly localized in liver, spleen and lung. Rare uptake of MNPs was observed in kidney, lymph node and thymus. No stains were observed in PBS-administered control tissues, indicating that no endogenous peroxidase activity interferes MNPs-peroxidase staining.

We next examined the cellular location of MNPs in liver, spleen and lung. After MNPs-peroxidase assay staining, tissue sections were further stained by H&E. As shown in Figure 3, MNPs were distributed mainly in Kuppfer macrophage cells in liver, alveolar macrophages in lung and macrophage peri-

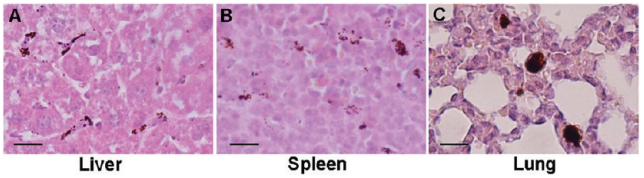

Figure 3. Dextran-coated MNPs were uptaken mainly by reticuloendothelial system (RES) in liver, spleen and lung. Tissue sections were first stained by MNPs-peroxidase assay and then counterstained with H&E to make cell structure more visible. (Scale bar = 50 μm.)

follicular areas in spleen, demonstrating that the accumulation of MNPs in these organs is caused mainly by reticuloendothelial cell uptake, which is consistent with previous reports.[30]

To validate the feasibility of MNPs-peroxidase assay staining in paraffin-embedded tissues, MNP-administered mice were sacrificed at 5 h postinjection and the main organs were collected and paraffin-embedded for MNPs-peroxidase staining. As shown in Figure 4, paraffin-embedded organs show a

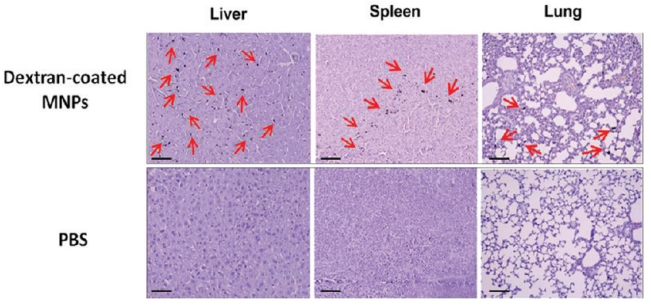

Figure 4. MNPs-peroxidase staining of paraffin-embedded liver, spleen, and lung from dextran-coated MNPs-administered mice (upper) or PBS-administered mice (lower). Arrows indicate stained MNPs. (Scale bar = 100 μm.)

distinct localization of MNPs. These results indicate that MNPs can be detected by the MNPs-peroxidase approach both in frozen and in paraffin-embedded organs. Importantly, although MNPs were subjected to xylene deparaffinization, ethanol rehydration and quenching endogeneous peroxidases in methanol, the peroxidase activity of MNPs has not been influenced, as evident in Figure 1C. We further showed that

dx.doi.org/10.1021/mp300033a | *Mol. Pharmaceutics* XXXX, XXX, XXX−XXX

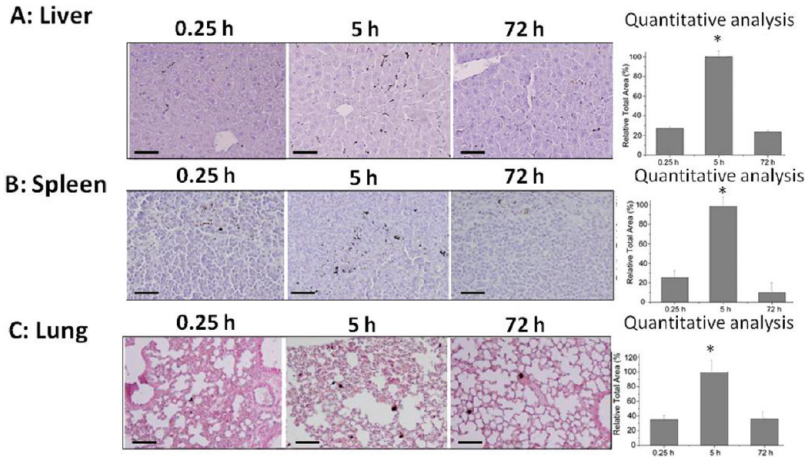

Figure 5. Organ clearance of dextran-coated MNPs. Liver, spleen, and lung were acquired from mice at 0.25, 5, and 72 h postinjection of 10 mg/kg of MNPs. Quantitative analysis of MNPs in liver, spleen, and lung was made using ImageJ software. *, $P < 0.05$ from the time point of 0.25 h postinjection of MNPs; $n = 4$ mice per group. (Scale bar = 100 μm.)

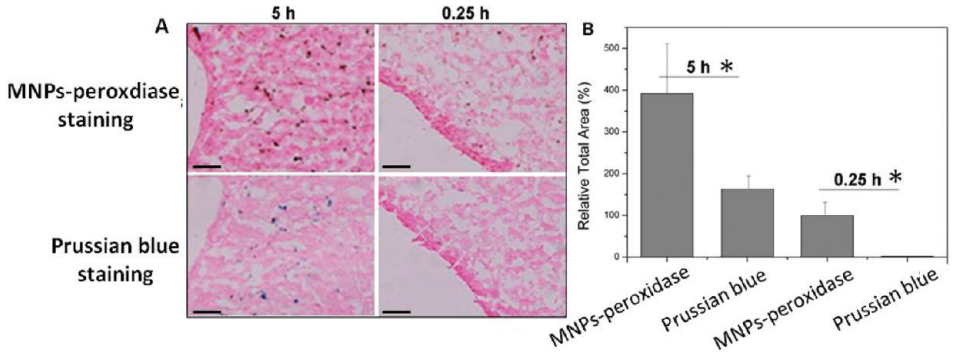

Figure 6. Comparison of the sensitivity of MNPs-peroxidase staining and Prussian blue staining. (A) Staining images of liver by MNPs-peroxidase staining or Prussian blue. Liver sections were acquired from mice at 0.25 and 5 h after intravenous injection of 10 mg/kg of dextran-coated MNPs. (B) Quantitative analysis was made using ImageJ software. *, $P < 0.05$. (Scale bar = 100 μm.)

administered MNPs at different sizes all can be visualized clearly in tissues (Supplementary Figure S3 in the Supporting Information), indicating that that there are no limitations to MNP sizes.

Organ Clearance of MNPs. Clearance of MNPs in organs was determined in dextran-coated MNPs-administered mice. The main organs were harvested at 0.25, 5, and 72 h postinjection, embedded in paraffin sections and cut at 5 μm for the subsequent histological staining. Ten representative slices were randomly chosen from each organ. After tissue staining by MNPs-peroxidase assay, the accumulated MNPs per area of these representative slices were analyzed by ImageJ. The error bars from these ten representative tissue slices are within 10%, indicating that the change of accumulated MNP slice by slice is not substantial in the same organ. Therefore, the measured MNPs of a random ten slices can totally represent the MNP accumulation in these organs. The final data were the means of four mice per group. As shown in Figure 5, the uptake of MNPs in liver, spleen and lung increased steadily from 0.25 to 5 h postinjection and then decreased from 5 to 72 h postinjection, indicating a rapid clearance.

Sensitivity Comparison with Prussian Blue Staining. Prussian blue staining is commonly used for iron oxide MNP staining in tissues.[12−14] However, the Prussian blue staining method is not sensitive enough when detecting low amounts of MNPs. In addition, the results are usually affected by the loosely bound endogenous ferric iron in tissues.[15] The MNPs-peroxidase approach does not have this issue because the endogenous iron exhibits little peroxidase activity.[1] We compared the sensitivity of MNPs-peroxidase staining and Prussian blue staining by detecting two sequential tissue sections using these two approaches. As shown in Figure 6, MNPs-peroxidase staining visualized two times more MNPs than Prussian blue staining at two sequential tissue sections. And when MNP amount in organs is too low to be detectable by Prussian blue staining, MNPs-peroxidase staining still can locate them out (Figure 6A, right column), suggesting a better detection sensitivity of MNPs-peroxidase approach than Prussian blue staining.

Detection of Administered Silica-Coated MNPs in Tissues. Silica has also been commonly used as coating materials for MNPs because silica coating provides an ideal platform for drug delivery.[31−33] We next examined the clearance of silica-coated MNPs by MNPs-peroxidase staining. Silica-coated MNPs at 10 mg/kg were first injected intravenously into the mouse. The mouse was then sacrificed at 0.25, 5 and 72 h postinjection, and the organs were harvested and embedded in paraffin sections. To quantify the accumulated MNPs in these tissues, ten representative tissue slices were randomly chosen from the same organ. After tissue staining by MNPs-peroxidase assay, the accumulated MNPs per area of these representative slices were analyzed by ImageJ. The

dx.doi.org/10.1021/mp300033a | Mol. Pharmaceutics XXXX, XXX, XXX−XXX

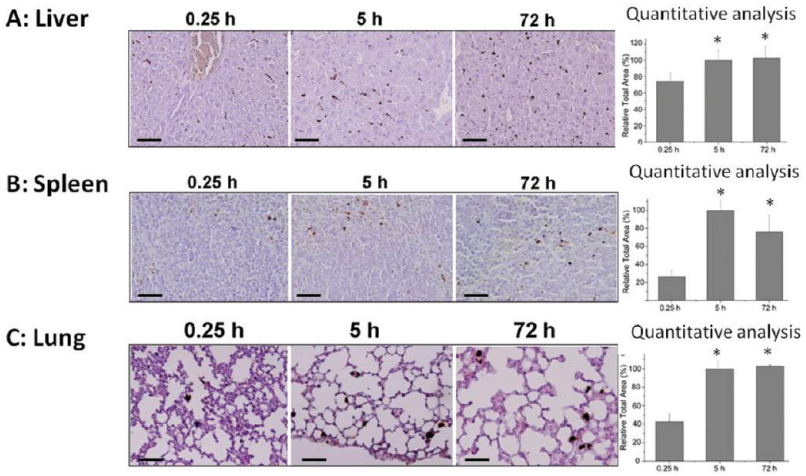

Figure 7. Organ clearance of silica-coated MNPs. Liver, spleen, and lung were acquired from mice at 0.25, 5, and 72 h postinjection of 10 mg/kg of MNPs. Quantitative analysis of MNPs in liver, spleen, and lung was made using ImageJ software. *, $P < 0.05$ from time point of 0.25 h postinjection of MNPs; $n = 4$ mice per group. (Scale bar = 100 μm.)

final data were the means of four mice per group. As shown in Figure 7, the uptake of silica-coated MNPs in liver, spleen and lung increased steadily from 0.25 to 72 h, suggesting a rather slow clearance of silica-coated MNPs from the body. The results are consistent with the previous reports which demonstrated that silica-coated nanoparticles were cleared out from the body over several days.[31]

DISCUSSION

Researchers employ numerous techniques to study MNP behavior in mice, including in vivo molecular imaging,[7−9] ex vivo organ biodistribution of indicator labeled nanoparticles following necropsy and histology staining.[34,35] The recent advance of commercially available small-animal molecular imaging instrumentation, such as single-photon emission computed tomography (SPECT), positron emission tomography (PET) and optical imaging, has enabled in vivo, dynamic, quantitative measurements of radio- or fluorophore-labeled MNPs in mouse models.[7−9] However, exogenous labeling generally changes the surface properties of MNPs and increases hydrodynamic diameter, which can interfere with their in vivo behavior. Thus developing an MNP intrinsic property-based method could offer the possibility to provide a real understanding of their behavior after administration into the body.

Previously, we reported for the first time that MNPs exhibit peroxidase activity that could catalyze the oxidation of peroxidase substrates to produce a color reaction,[1] and since that time numerous papers on this topic have been published.[16−21] In this present study, we are developing an ex vivo MNPs detection method based on their intrinsic peroxidase activity. This MNPs-peroxidase approach was designed to visualize administered MNPs in tissues by catalyzing the oxidation of peroxidase substrates to form a color deposition at the site of MNPs. We first established that the peroxidase activity of MNPs remained stable after incubation in serum at 37 °C or in organic solution at 25 °C (Figure 1), which is necessary because an intrinsic property under consideration for MNP detection in mice must be sufficiently stable when MNPs are in circulation in organs and throughout their passage across the in vitro tissue staining process that involves organic solution incubation. We next demonstrated that commercially available MNPs exhibited similar peroxidase activity with laboratory synthesized MNPs at the same size (Supplementary Figure S1 in the Supporting Information), illustrating that there are no limitations to MNP sources. Thereafter, main organs from MNP-administered mice were collected for MNPs-peroxidase assay staining. As shown in Figures 2 and 4, the administered MNPs are evident in both frozen and paraffin tissue sections, confirming the feasibility of visualizing MNPs in tissues by employing their intrinsic peroxidase activity. The endogenous iron species were not visualized with the same staining process when peroxidase substrate was added (Figures 2 and 4, lower) because the endogenous iron species do not exhibit intrinsic peroxidase activity due to the differences of the mineral phase composition. We then showed that administered MNPs at different sizes all can be visualized clearly in tissues (Supplementary Figure S3 in the Supporting Information), indicating that that there are no limitations to MNP sizes. Finally, the MNP clearance study provided quantitative information on MNP accumulation over time in several main organs (Figure 5), which further confirms the feasibility of the MNPs-peroxidase approach in MNP detection in tissues. Prussian blue staining images show obviously less sensitive measurement for MNPs as compared with the MNPs-peroxidase approach in sequential tissue sections (Figure 6), which can be explained by the highly effective catalytic activity of MNPs.[1]

CONCLUSION

In conclusion, we have demonstrated the feasibility of using the MNPs-peroxidase approach to detect MNPs in mice by employing their intrinsic peroxidase-mimicking activity. As shown above, the MNP biodistribution and clearance in mouse models were determined conveniently by visualizing and quantifying MNP localization within the main organs using their peroxidase activity. The developed MNPs-peroxidase approach is more sensitive when compared with the traditional Prussian blue staining method because of the highly effective catalytic activity of MNPs. Importantly, as this approach avoids complex and costly labeling with exogenous indicators, this reduces false background signals and provides the possibility to understand the real behavior of MNPs in mice and thus has significant implications for the clinical translation of MNPs.

dx.doi.org/10.1021/mp300033a | *Mol. Pharmaceutics* XXXX, XXX, XXX−XXX

Presumably, other nanoparticles having intrinsic peroxidase activity could also be considered.

■ ASSOCIATED CONTENT

Supporting Information

Additional experimental details and related figures. This material is available free of charge via the Internet at http://pubs.acs.org.

■ AUTHOR INFORMATION

Corresponding Author

*X.Y.: Institute of Biophysics, Chinese Academy of Sciences, National Laboratory of Biomacromolecules, Datun Road No. 15, Beijing 100101, China; e-mail, yanxy@ibp.ac.cn; tel, +86 10 6488 8583; fax, +86 10 6488 8584. M.L.: e-mail, mmliang@moon.ibp.ac.cn; tel, +86 10 6488 8503; fax, +86 10 6488 8584.

Notes

The authors declare no competing financial interest.

■ ACKNOWLEDGMENTS

This work was partially supported by grants from the National Science and Technology Major Project (2012ZX10002009-016), 973 Program (2011CB933500, 2011CB915502, 2012CB934993), the Knowledge Innovation Program of the Chinese Academy of Sciences (KJCX2-YW-M15), and the National Defense Science and Technology Innovation Fund of Chinese Academy of Sciences (CXJJ-11-M61).

■ REFERENCES

(1) Gao, L.; Zhuang, J.; Nie, L.; Zhang, J.; Zhang, Y.; Gu, N.; Wang, T.; Feng, J.; Yang, D.; Perrett, S.; Yan, X. Intrinsic peroxidase-like activity of ferromagnetic nanoparticles. *Nat. Nanotechnol.* **2007**, *2*, 577−583.

(2) Jain, T. K.; Morales, M. A.; Sahoo, S. K.; Leslie-Pelecky, D. L.; Labhasetwar, V. Iron oxide nanoparticles for sustained delivery of anticancer agents. *Mol. Pharmaceutics* **2005**, *2*, 194−205.

(3) Mornet, S.; Vasseur, S.; Grasset, F.; Duguet, E. Magnetic nanoparticle design for medical diagnosis and therapy. *J. Mater. Chem.* **2004**, *14*, 2161−2175.

(4) Dobson, J. Magnetic nanoparticles for drug delivery. *Drug Dev. Res.* **2006**, *67*, 55−60.

(5) Choi, H. S.; Liu, W.; Liu, F.; Nasr, K.; Misra, P.; Bawendi, M. G.; Frangioni, J. V. Design considerations for tumour-targeted Nanoparticles. *Nat. Nanotechnol.* **2010**, *5*, 42−47.

(6) Lee, P. W.; Hsu, S. H.; Wang, J. J.; Tsai, J. S.; Lin, K. J.; Wey, S. P.; Chen, F. R.; Lai, C. H.; Yen, T. C.; Sung, H. W. The characteristics, biodistribution, magnetic resonance imaging and biodegradability of superparamagnetic core-shell nanoparticles. *Biomaterials* **2010**, *31*, 1316−24.

(7) Glaus, C.; Rossin, R.; Welch, M. J.; Bao, G. *In vivo* evaluation of (64)Cu-labeled magnetic manoparticles as a dual-modality PET/MR imaging agent. *Bioconjugate Chem.* **2010**, *21*, 715−722.

(8) Ge, Y. Q.; Zhang, Y.; He, S. Y.; Nie, F.; Teng, G. J.; Gu, N. Fluorescence modified chitosan-coated magnetic nanoparticles for high-efficient cellular imaging. *Nanoscale Res. Lett.* **2009**, *4*, 287−295.

(9) Devaraj, N. K.; Keliher, E. J.; Thurber, G. M.; Nahrendorf, M.; Weissleder, R. ^{18}F Labeled nanoparticles for *in vivo* PET-CT imaging. *Bioconjugate Chem.* **2009**, *20*, 397−401.

(10) Lee, P. W.; Hsu, S. H.; Wang, J. J.; Tsai, J. S.; Lin, K. J.; Wey, S. P.; Chen, F. R.; Lai, C. H.; Yen, T. C.; Sung, H. W. The characteristics, biodistribution, magnetic resonance imaging and biodegradability of superparamagnetic core-shell nanoparticles. *Biomaterials* **2010**, *31*, 1316−1324.

(11) Cole, A. J.; David, A. E.; Wang, J. X.; Galban, C. J.; Yang, V. C. Magnetic brain tumor targeting and biodistribution of long-circulating PEG-modified, cross-linked starch-coated iron oxide nanoparticles. *Biomaterials* **2011**, *32*, 6291−6301.

(12) Schroeter, M.; Saleh, A.; Wiedermann, D.; Hoehn, M.; Jander, S. Histochemical detection of ultrasmall superparamagnetic iron oxide (USPIO) contrast medium uptake in experimental brain ischemia. *Magn. Reson. Med.* **2004**, *52*, 403−406.

(13) Yu, L.; Scherlag, B. J.; Dormer, K.; Nguyen, K. T.; Pope, C.; Fung, K. M.; Po, S. S. Autonomic Denervation With Magnetic Nanoparticles. *Circulation* **2010**, *122*, 2653−2659.

(14) Raju, H. B.; Hu, Y.; Vedula, A.; Dubovy, S. R.; Goldberg, J. L. Evaluation of Magnetic Micro- and Nanoparticle Toxicity to Ocular Tissues. *PLoS One* **2011**, *6*, e17452.

(15) Poss, K. D.; Tonegawa, S. Heme oxygenase 1 is required for mammalian iron reutilization. *Proc. Natl. Acad. Sci. U.S.A.* **1997**, *94*, 10919−10924.

(16) Wei, H.; Wang, E. Fe_3O_4 magnetic nanoparticles as peroxidase mimetics and their applications in H_2O_2 and glucose detection. *Anal. Chem.* **2008**, *80*, 2250−2254.

(17) Song, Y. J.; Qu, K. G.; Zhao, C.; Ren, J. S.; Qu, X. G. Graphene Oxide: Intrinsic Peroxidase Catalytic Activity and Its Application to Glucose Detection. *Adv. Mater.* **2010**, *22*, 2206−2210.

(18) Luo, W.; Zhu, L. H.; Wang, N.; Tang, H. Q.; Cao, M. J.; She, Y. B. Efficient Removal of Organic Pollutants with Magnetic Nanoscaled BiFeO(3) as a Reusable Heterogeneous Fenton-Like Catalyst. *Environ. Sci. Technol.* **2010**, *44*, 1786−1791.

(19) Zhang, J. B.; Zhuang, J.; Gao, L. Z.; Zhang, Y.; Gu, N.; Feng, J.; Yang, D. L.; Zhu, J. D.; Yan, X. Y. Decomposing phenol by the hidden talent of ferromagnetic nanoparticles. *Chemosphere* **2008**, *73*, 1524−1528.

(20) Zhu, M. Y.; Diao, G. W. Synthesis of porous Fe3O4 nanospheres and its application for the catalytic degradation of xylenol orange. *J. Phys. Chem. C* **2011**, *115*, 18923−18934.

(21) Zhai, Y. M.; Zhai, J. F.; Zhou, M.; Dong, S. J. Ordered magnetic core-manganese oxide shell nanostructures and their application in water treatment. *J. Mater. Chem.* **2009**, *19*, 7030−7035.

(22) Deng, H.; Li, X. L.; Peng, Q.; Wang, X.; Chen, J. P.; Li, Y. D. Monodisperse magnetic single-crystal ferrite microspheres. *Angew. Chem., Int. Ed.* **2005**, *44*, 2782−2785.

(23) Yan, F.; Xu, H.; Anker, J.; Kopelman, R.; Ross, B.; Rehemtulla, A.; Reddy, R. Synthesis and characterization of silica-embedded iron oxide nanoparticles for magnetic resonance imaging. *J. Nanosci. Nanotechnol.* **2004**, *4*, 72−76.

(24) Yiu, H. H. P. Engineering the multifunctional surface on magnetic nanoparticles for targeted biomedical applications: a chemical approach. *Nanomedicine* **2011**, *6*, 1429−1446.

(25) Lacava, L. M.; Lacava, Z. G. M.; Da Silva, M. F.; Silva, O.; Chaves, S. B.; Azevedo, R. B.; Pelegrini, F.; Gansau, C.; Buske, N.; Sabolovic, D.; Morais, P. C. Magnetic resonance of a dextran-coated magnetic fluid intravenously administered in mice. *Biophys. J.* **2001**, *80*, 2483−2486.

(26) Babes, L.; Denizot, B.; Tanguy, G.; Le Jeune, J. J.; Jallet, P. Synthesis of iron oxide nanoparticles used as MRI contrast agents: A parametric study. *J. Colloid Interface Sci.* **1999**, *212*, 474−482.

(27) Dias, A. M. G. C.; Hussain, A.; Marcos, A. S.; Roque, A. C. A. A biotechnological perspective on the application of iron oxide magnetic colloids modified with polysaccharides. *Biotechnol. Adv.* **2011**, *29*, 142−155.

(28) Harisinghani, M. G.; Saini, S.; Weissleder, R.; Halpern, E. F.; Schima, W.; Rubin, D. L.; Stillman, A. E.; Sica, G. T.; Small, W. C.; Hahn, P. F. Differentiation of liver hemangiomas from metastases and hepatocellular carcinoma at MR imaging enhanced with blood-pool contrast agent Code-7227. *Radiology* **1997**, *202*, 687−691.

(29) Massla, S. P.; Stark, J.; Letbette,r, D. S. Surface immobilized dextran limits cell adhersion and spreading. *Biomaterials* **2000**, *21*, 2253−2261.

(30) Ma, H. L.; Xu, Y. F.; Qi, X. R.; Maitani, Y.; Nagai, T. Superparamagnetic iron oxide nanoparticles stabilized by alginate: pharmacokinetics, tissue distribution, and applications in detecting liver cancers. *Int. J. Pharm.* **2008**, *354*, 217−226.

(31) Gupta, A. K.; Naregalkar, R. R.; Vaidya, V. D.; Gupta, M. Recent advances on surface engineering of magnetic iron oxide nanoparticles and their biomedical applications. *Nanomedicine* **2007**, *2*, 23−39.
(32) Wu, H. X.; Liu, G.; Zhang, S. J. Biocompatibility, MR imaging and targeted drug delivery of a rattle-type magnetic mesoporous silica nanosphere system conjugated with PEG and cancer-cell-specific ligands. *J. Mater. Chem.* **2011**, *21*, 3037−3045.
(33) Vallet-Regi, M.; Balas, F.; Arcos, D. Mesoporous materials for drug delivery. *Angew. Chem., Int. Ed.* **2007**, *46*, 7548−7558.
(34) Kumar, R.; Roy, I.; Ohulchanskyy, T. Y.; Goswami, L. N.; Bonoiu, A. C.; Bergey, E. J.; Tramposch, K. M.; Maitra, A.; Prasad, P. N. Covalently dye-linked, surface-controlled, and bioconjugated organically modified silica nanoparticles as targeted probes for optical imaging. *ACS Nano* **2008**, *2*, 449−456.
(35) Torres, R.; Tavaré, R.; Paul, R. L.; Jauregui-Osoro, M.; Protti, A.; Glaria, A.; Varma, G.; Szanda, I.; Blower, P. J. Synthesis of ^{64}Cu(II)-bis(dithiocarbamatebisphosphonate) and its conjugation with superparamagnetic iron oxide nanoparticles: in vivo evaluation as dual-modality PET-MRI agent. *Angew. Chem., Int. Ed.* **2011**, *50*, 5509−5513.